Microsc. Microanal. 4, 226–234, 1998

Microscopy AND Microanalysis

High-Temperature In Situ Straining Experiments in the High-Voltage Electron Microscope

Ulrich Messerschmidt,[1]* Dietmar Baither,[1] Martin Bartsch,[1] Bernd Baufeld,[1] Bert Geyer,[1] Susanne Guder,[1] Anna Wasilkowska,[2] Aleksandra Czyrska-Filemonowicz,[2] Masaharu Yamaguchi,[3] Michael Feuerbacher,[4] and Knut Urban[4]

[1]*Max Planck Institute of Microstructure Physics, Weinberg 2, Halle/Saale D-06120, Germany*
[2]*Faculty of Metallurgy and Materials Science, University of Mining and Metallurgy, Al. Mickiewicza 30, Krakow 30-059, Poland*
[3]*Department of Metal Science and Technology, Kyoto University, Kyoto 606-01, Japan*
[4]*Institute of Solid State Research, Jülich Research Centre, Jülich D-52425, Germany*

Abstract: Design rules are described here for high-temperature straining stages for transmission electron microscopy. Temperatures above 1000°C can be attained by electron bombardment of the specimen grips. Thermal equilibrium can be reached in a short time by carrying off the heat by water cooling. Some applications of this stage are described. Ferroelastic deformation was observed at 1150°C in t′ and partially stabilized zirconia, which changes the microstructure for successive dislocation plasticity. In the oxide-dispersion-strengthened alloy INCOLOY MA 956, dislocations are impeded by oxide particles and move smoothly between the particles. At high temperatures, both the resting and traveling times control the average dislocation velocity. In $MoSi_2$ single crystals of a soft orientation, dislocations with 1/2⟨111⟩ Burgers vectors are created in localized sources and move on {110} planes in a viscous manner. The dislocations in Al-Pd-Mn single quasicrystals are oriented in preferred crystallographic directions and move in a viscous way as well. On the basis of in situ observations, conclusions are drawn for interpreting macroscopic deformation behavior at high temperatures.

Key words: high-voltage electron microscopy, in situ straining experiments, high-temperature mechanical properties, dislocations, zirconia, oxide-dispersion strengthened alloys, molybdenum disilicide, quasicrystals

Introduction

In situ straining experiments using a transmission electron microscope (TEM) may reveal details of the mechanisms of plastic deformation that other methods cannot directly provide. For these experiments, a high-voltage electron microscope (HVEM) has two advantages compared to conventional microscopes: its large penetration power allows the observation of relatively thick specimens, thus the behavior of individual dislocations resembles that in bulk specimens. In addition, it provides adequate space in the specimen chamber for installing elaborate in situ stages. Investigation of materials for future technologies often requires temperatures above 1000°C. In the present report, we show that it is

Received March 1, 1998; accepted June 16, 1998.

Dietmar Baither's present address is Institute of Metals Research, Münster University, Wilhelm-Klemm-Str. 10, Münster D-48149, Germany.
Bernd Baufeld's present address is Institute of Materials Science, Martensstrasse 5, Erlangen D-91058, Germany.
*Corresponding author

difficult to reach these temperatures by resistance heating of the specimen grips. A way around this is the application of electron bombardment, which was introduced in the design of high-temperature electron microscopy stages by Fujita and Komatsu (1983). We describe here the physical basis of designing straining stages for high temperatures, and some applications of a stage presently operating at up to 1150°C are demonstrated on ceramic, metallic, and quasicrystalline materials.

Design Rules for High-Temperature Straining Stages

High-temperature straining stages for a transmission electron microscope must fulfill the following requirements. To reduce the image shift, the stage has to reach thermal equilibrium quickly. The mechanical design should be stable and the maximum force should exceed 10 N to deform materials of high strength.

There are two philosophies for the thermal design. The first one, described in detail by Valle et al. (1982), tries to minimize heat losses so that a cooling system can be avoided. This is difficult to achieve in the restricted space that is usually available in the specimen chambers of electron microscopes. Therefore, another way is described here. It consists of producing the heat necessary to reach high temperatures and to carry off this heat through a water cooling system. The first step in the thermal design is the estimation of heat losses. Heat losses are due to heat conduction and radiation. Heat flow N by conduction is given by

$$N = (T_1 - T_2)\ \lambda\ A/L, \qquad (1)$$

where T_1 and T_2 are the temperatures of the hot and cold ends of the heat conducting parts, λ is the thermal conductivity, and A and L are the cross section and length of the parts. Heat conduction problems appear particularly in top-entry straining stages where parts have to be loaded in bending. The maximum load of a bending bar is

$$F_m = \sigma_m\ W/L, \qquad (2)$$

with σ_m being the maximum stress of the material, and W the section modulus. As an example, $W = 0.05\ D^3$ and $A = 0.23\ D^2$ for cylindrical tubes of diameter D and a wall thickness of 0.08 D. A good lever has a large value of

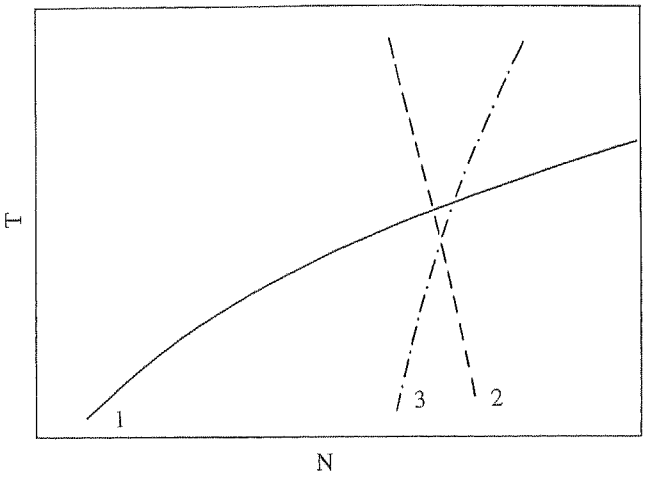

Figure 1. Schematic plot of the temperature dependence of heat losses (curve 1) and of the power of resistance heaters from Superkanthal (curve 2) and from metals and SiC (curve 3).

$$F_m\ (T_1 - T_2)/N = \sigma_m\ W/(\lambda\ A) \cong 0.2\ \sigma_m\ D/\lambda, \qquad (3)$$

which can be reached by appropriately selecting the right material and a large value of D. This leads to a large L if a certain value of N is wanted.

Heat loss by radiation can be estimated by the Stefan-Boltzmann law:

$$N_{12} = \sigma\ A_1\ \varepsilon_e\ (T_1^4 - T_2^4), \qquad (4)$$

with $\sigma = 5.7 * 10^{-8}$ W m^{-2} K^{-4} and the average emissivity

$$\varepsilon_e = \varepsilon_1\ \varepsilon_2/[1 - (1 - \varepsilon_2)(1 - (A_1/A_2)\ \varepsilon_1)].$$

Subscripts 1 and 2 refer to the radiating and reflecting surfaces. In practice, correct values of the radiating losses are obtained for $\varepsilon \cong 0.5$, or larger, as the theoretical values of the emissivity of clean polished surfaces are reduced by contamination. Heat loss by radiation can be reduced by using radiation shields. One shield may reduce the loss by 50%. Again, the theoretical values are not attained in practice. Usually, there is no space in the microscope for more than one shield.

Owing to the 4th power of T_1 in Equation (4), the heat losses increase strongly with increasing T_1, particularly at high temperatures, as schematically shown by curve 1 in Figure 1. On the other hand, the maximum power density of resistance heating materials depends only slightly on temperature. As also shown in Figure 1, it decreases with increasing temperature for Superkanthal (curve 2), but increases for metals and SiC (curve 3). Nevertheless, the maxi-

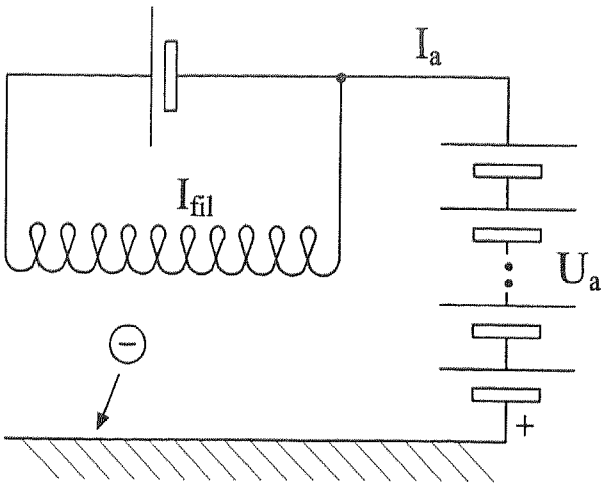

Figure 2. Circuit diagram of electron bombardment heating.

mum power density at 1000°C is on the order of 10 W cm^{-2} for the relevant materials. The surface of the heating wire is usually not larger than the radiating surface of the hot parts of the stage. This makes curve 1 cross one of curves 2 or 3 at about 1000°C, i.e., it is relatively easy to design heating stages using resistance heating for temperatures below 1000°C, but it becomes increasingly difficult for higher temperatures.

As shown by Fujita and Komatsu (1983), the problem can be solved by heating the specimen grips by electron bombardment. Figure 2 demonstrates the principle. The specimen grips are electrically at ground. A filament is connected to a negative voltage U_a. The filament is heated by the current I_{fil} and emits an electron current I_a. The electrons hit the grips, heating them with the power $N = U_a I_a$, in addition to the heat radiating from the filament. The saturation current density of filaments strongly increases with the filament temperature. For tungsten filaments, a current density of 0.7 A cm^{-2} is obtained at a temperature where the vapor pressure amounts to 5.4 * 10^{-7} torr, and the evaporation rate to 3.9 * 10^{-9} g cm^{-2} s^{-1}. This may be considered a maximum current density with the vacuum only slightly deteriorating and the filaments having a long life. In order not to limit the current density by space charge effects, the distance between the filament and the anode (ground) must be small. This, however, increases the possibility of uncontrolled discharges.

Since anode voltages U_a on the order of 1 kV can be used, much heat can be produced (~100 W) within a relatively small volume yielding high temperatures. To avoid damage to the microscope as well as to reach thermal equilibrium in a short period of time, the heat should be carried off by means of a water cooling system. The cooling system may cause specimen vibrations if the water flow is not laminar. The condition to be met is that Reynold's number (Re) is

$$\mathrm{Re} = w\, l/\nu < 2300, \tag{5}$$

with w being the flow velocity, l a characteristic length, e.g., the diameter of a tube, and ν the kinematic viscosity (=0.7 mm^2 s^{-1} for water). For example, the flow in a tube of 2 mm in diameter will be laminar if the flow rate is <2 cm^3 s^{-1}, corresponding to 40 W for a temperature increase of 5K of the cooling liquid. In addition to the character of flow, the transfer of the heat from the wall of the heat exchanger to the cooling liquid has to be considered. It is governed by

$$N = \alpha\, A\, (T - T_w). \tag{6}$$

Here, α is the heat transfer number, A, the area of the inner tube surface, T, the temperature of the wall, and T_w, that of the cooling liquid. α shows an intermediate dependence on the thermal conductivity of the cooling liquid and a weak dependence on the other parameters as the density and specific heat of the cooling liquid, the diameter and length of the tube, and the flow velocity. Thus, there is little freedom to manipulate α, but one has to choose a sufficiently large contact area A. A number of experiments were performed with small heat exchangers consisting of copper lamellae with 0.3-mm-wide slits between them, and with glass windows to observe the water flow, as well as with electron microscope specimens attached to them to check the specimen vibrations in the electron microscope. These experiments showed that the contact area should be larger than 10 mm^2 W^{-1} to avoid specimen vibrations from water boiling inside the heat exchangers.

An important parameter of the mechanical design of the straining unit is its elastic stiffness. A hard stage promotes stability of crack growth if the specimen has a crack. However, the load decreases when the specimen deforms, which is sometimes not wanted. Nevertheless, a hard stage is usually better than a soft one, particularly if it implies the facility of measuring the load. A severe problem is the drive of the deformation. For a double-tilting straining stage, the drive mechanism should be installed on the tilted part. This is only possible if the drive mechanism is small enough. On the other hand, the drive should exert a large force on the specimen and yield a sufficient elongation, including com-

Table 1. Different Drives of Equal Size (6 mm in diameter and 10 mm in length) for Straining Stages

	Maximum force (N)	Maximum elongation (μm)	Energy density (J m^{-3})
Piezo-electric	315	5	5600
Thermal expansion	1800	48	340,000
Hydraulic	110	480	380,000

pensation for the thermal expansion of the specimen. A smooth action of the drives can be achieved by using piezo-electric actuators, thermal expansion of stainless steel rods, and hydraulic drives with metal bellows. Table 1 compares the maximum force and elongation and the energy density of these drive principles for cylinders of equal size. It shows that the piezo-electric drive has a low-energy density and is therefore not suited for electron microscope straining stages. Thermal and hydraulic drives have similar energy densities. The hydraulic drive is sensitive to vacuum pumping of the microscope column and does not have a well-defined stiffness. Thus, thermal expansion of a stainless steel rod is certainly best suited for driving straining stages.

The described estimations were used to design a top-entry straining stage for an HVEM for temperatures above 1000°C. It is described in detail by Messerschmidt and Bartsch (1994). Each specimen grip carries a separate filament for electron bombardment heating. The temperatures are measured by W-Re 3/25 thermocouples. Grip temperatures of 1250°C are obtained by applying an electron current of about 65 mA at 700 V. Higher temperatures should still be possible. The heat is carried away by a water cooling system. The deformation is driven by the thermal expansion of a stainless steel rod. A power of 6 W causes a displacement of about 1 mm of the movable grip. The force is measured by a full bridge of semiconducting strain gauges. The whole stage is controlled by use of a personal computer. In the following sections, recent applications of the stage are described.

In Situ Straining Experiments on Tetragonal Zirconia Single Crystals

Because of its strong precipitation hardening (e.g., Heuer et al., 1989), zirconia containing precipitates of the tetragonal

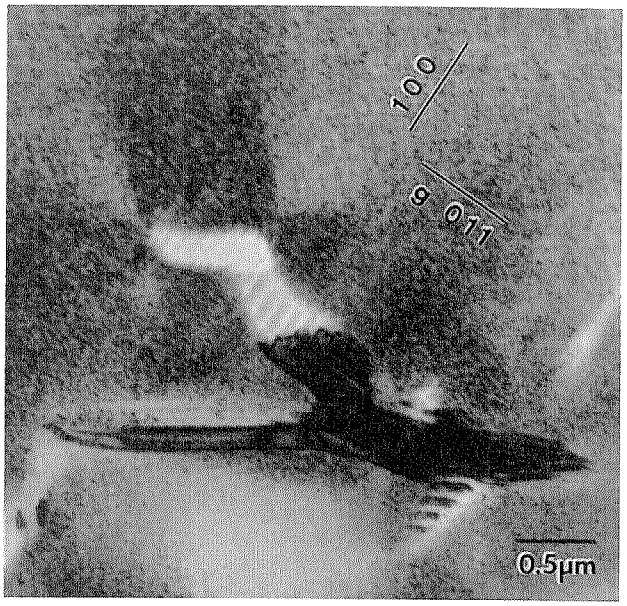

Figure 3. Microstructure of yttria partially stabilized zirconia partly transformed by ferroelastic deformation during in situ straining in the HVEM at 1150°C. The micrographs in this report were taken by the high-order bright-field technique. Two directions in the image plane are indicated.

phase (partially stabilized zirconia, PSZ) is a promising material for structural applications at high temperatures. Metastable tetragonal zirconia, so-called t′-zirconia, has a microstructure consisting of tetragonal domains alternately stacked in colonies. Colonies of different orientations of the domains fill the entire crystal volume. t′-zirconia exhibits ferroelastic deformation under load (e.g., Chan et al., 1991). In situ straining experiments were performed on this material at a specimen temperature of 1150°C (Baufeld et al., 1997). They proved the process of switching individual domains to result in a tetragonal single crystal, with the c-axes of the tetragonal domains situated at a unique orientation.

Similar experiments were performed on partially stabilized zirconia single crystals (Baufeld et al., 1995). This material contains tetragonal precipitates of a domain structure similar to that in t′-zirconia. The size of the precipitates shows a bimodal distribution as demonstrated in Figure 3. A few large precipitates consist of one or a few colonies of wide domains. Most precipitates are very small and form a so-called tweed structure. The individual precipitates of the tweed structure have a domain structure on a smaller scale. During loading, the strong diffraction contrast of the domain structure disappears owing to ferroelastic domain switching analogous to t′-zirconia. This is shown by the

bright part in the large precipitate in the center of the figure and by the border between the dark and less dark regions in the tweed structure. During further deformation, large domains switch instantaneously while the border between the transformed and the untransformed regions of the tweed structure moves smoothly. Ferroelastic domain switching had not been previously observed in partially stabilized zirconia. Because of the small resulting strain, it is difficult to detect in the deformation curve. The result was only recently confirmed by an X-ray study by Kiguchi (1997). Domain switching is of great consequence to successive plastic deformation as it changes the microstructure which the gliding dislocations experience. In the untransformed structure, the dislocations have to penetrate colonies of domains with alternating directions of their c-axes, which causes a strong friction due to the stacking faults—these have to be produced in at least one set of domains. After ferroelastic transformation, however, most precipitates show a uniform orientation of their c-axes, which reduces their friction drastically. These processes are described in more detail by Messerschmidt et al. (1997).

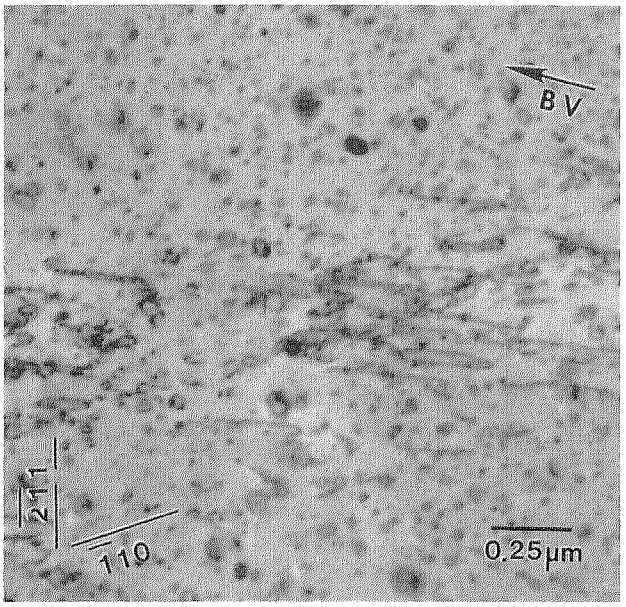

Figure 4. Dislocations moving during in situ deformation of the ODS alloy INCOLOY MA 956 at room temperature. The traces of the {110} slip planes run horizontally. In this and the following figures, BV indicates the projection of the Burgers vector.

Dislocation Dynamics in the Oxide-Dispersion Strengthened Alloy MA 956

The creep resistance of high-temperature materials can be drastically improved by the incorporation of a fine dispersion of oxide particles forming so-called oxide-dispersion strengthened alloys (ODS alloys). The particles are not cut by the dislocations. The flow stress at room temperature is therefore determined by the Orowan process. At high temperatures, the dislocations can pass the dispersoids by climb. Nevertheless, the creep rate is reduced by several orders of magnitude by incorporating the oxide particles. According to Srolovitz et al. (1984) and Arzt and Wilkinson (1986), this effect is due to an attractive interaction between the dislocations and the particles, which pins the dislocations at the exit side of the particles. The creep rate is determined by the thermally activated detachment of the dislocations from the pinned configurations.

In order to observe the dynamic behavior of dislocations in an ODS alloy, in situ straining experiments were performed for the first time on the ferritic ODS alloy INCOLOY MA 956 at room temperature, and between 640°C and 970°C. The microstructure and the macroscopic deformation behavior of this material are described by Schuster et al. (1995). Figure 4 shows dislocations on {110} planes under load during deformation at room temperature. Note that the slip plane is steeply inclined with respect to the image plane. The dislocations are pinned by the particles. As expected from the size and density of the oxide particles, the obstacle spacing is approximately 100 nm. Many dislocation loops appear within the region of the slip band. It cannot be decided whether they are Orowan loops created by the dislocations when bypassing the particles, or debris produced by the double-cross slip process. Video records show that the dislocations jump over longer distances than those between the particles on the slip plane, in accordance with the athermal character of the Orowan process.

At high temperatures, the configurations of resting dislocations are still determined by pinning due to the oxide particles, as demonstrated in Figure 5 for a temperature of 700°C. Some dislocations show strongly bowed-out segments, others are only weakly curved. The obstacle distance is slightly larger than the distance calculated from the size and concentration of the dispersoids. Qualitatively, at higher temperatures the situation is similar, as shown in Figure 6. Between their stable positions, the dislocations move continuously at velocities of fractions of 1 μm/sec. During their motion, the dislocations are only smoothly

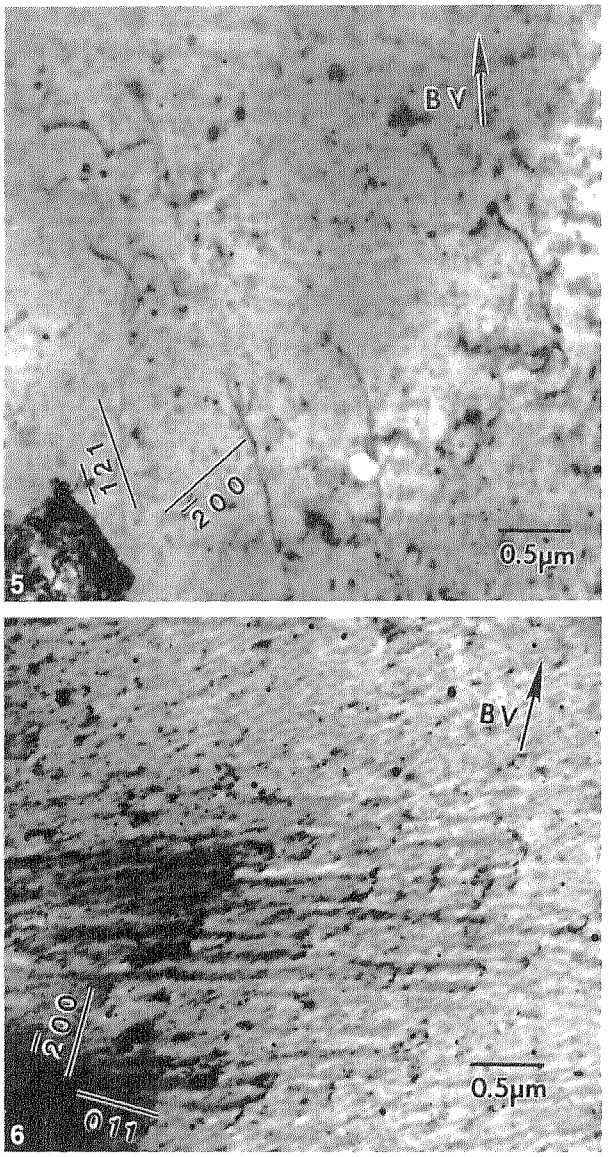

Figure 5. Dislocations moving during in situ deformation of INCOLOY MA 956 at about 700°C. The traces of the {123} slip planes run horizontally.

Figure 6. Dislocations moving during in situ deformation of INCOLOY MA 956 at about 970°C. The traces of the {123} slip planes run horizontally.

curved. They bow out again after being pinned by a strong obstacle configuration. The waiting times in the pinned state and the traveling times between these states are of the same order of magnitude. Thus, two processes seem to control the dislocation motion, viz., the thermally activated detachment from oxide particles, and a friction mechanism during motion. The friction mechanism presumably is connected with diffusion processes of trace elements that give rise to solution hardening at low temperatures. At high temperatures, they may form atmospheres that are dragged by the moving dislocations. The behavior of dislocations does not fit that expected from the current theory. In particular, the friction process, which is clearly proven by the dynamic behavior of dislocations, has not been considered until now. Quantitative evaluation of the micrographs and video recordings will reveal further details of the processes.

Dislocation Motion in $MoSi_2$ Single Crystals

Candidates promising to fill the gap between conventional high-temperature metals and structural ceramics are materials constructed on the basis of $MoSi_2$. To understand the mechanical properties of the composites under discussion, knowledge of the processes of plastic deformation of the $MoSi_2$ matrix is desirable. $MoSi_2$ has a tetragonal crystal structure with a large c/a ratio. Consequently, $MoSi_2$ exhibits a number of different slip systems and shows a strong plastic anisotropy (see, e.g., Ito et al., 1995). Like many intermetallic compounds, some of the slip systems show an anomalous temperature dependence of the flow stress.

As the processes controlling dislocation mobility are not well understood, in situ straining experiments were recently performed on $MoSi_2$ single crystals between about 900°C and 990°C. Because of the brittleness of the material at room temperature and at the deformation temperature, these experiments put high demands on specimen preparation. In addition, the starting crystals were predeformed in compression, introducing some dislocations to increase the toughness. The [201] direction chosen for the loading axis is a soft orientation, so dislocations of $1/2\langle 111\rangle$ Burgers vectors are activated on {110} planes. During loading, sudden load drops were accompanied by the formation of stacking faults of the Frank type. Later on, the dislocations of $1/2\langle 111\rangle$ Burgers vectors started to move. These were created by localized sources. An intermediate state is shown in Figure 7. The resting dislocations are very straight and in orientation parallel to $\langle 110]$ and $\langle 331]$, i.e., they are of 60° or edge character. During their viscous motion, they may assume a curved shape. Owing to the generation of dislocations in localized sources, planar slip dominates. The collective motion of many dislocations on the same slip plane may cause serrated yielding observed in the respective temperature range of the flow stress maximum. Frequently,

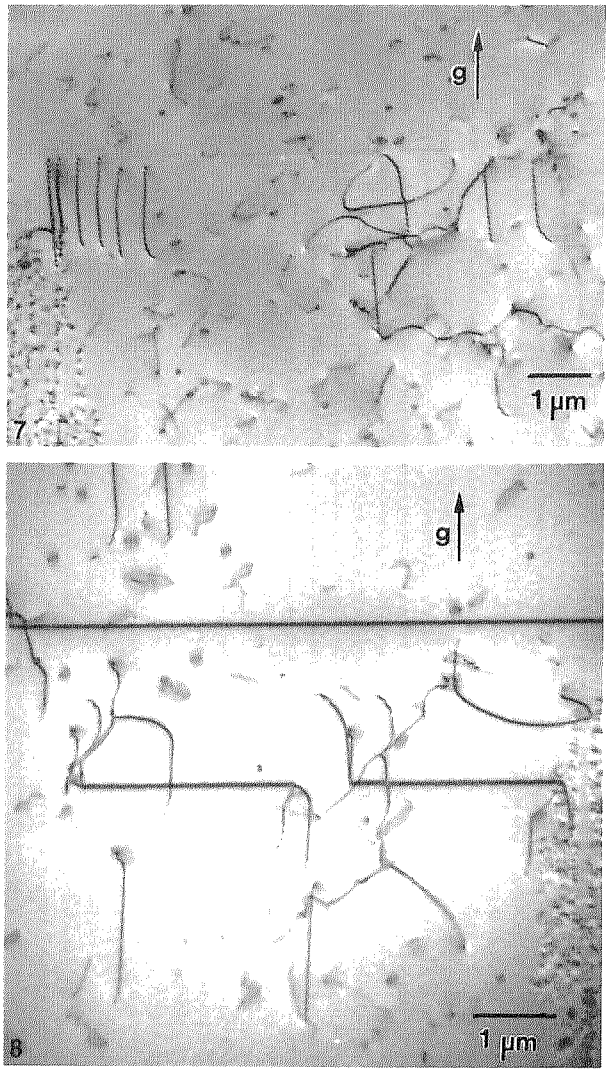

Figure 7. Dislocations moving away from a localized dislocation source during in situ deformation at about 990°C of an $MoSi_2$ single crystal. 1/2⟨111⟩ Burgers vectors. The traces of the {110} slip planes run horizontally. Foil plane (010), g-vector [200].

Figure 8. Long, straight defects oriented along ⟨100⟩ formed during in situ deformation of an $MoSi_2$ single crystal at about 990°C. Foil plane (010), g-vector [200].

dislocations moving on intersecting slip planes form a very straight common segment in the [001] direction of the intersecting planes, as shown in Figure 8. The character of these reaction products has not yet been determined. The shape of the dislocations of 1/2⟨111⟩ Burgers vectors and their mode of motion point to an intrinsic mechanism controlling the dislocation mobility. They do not agree with a locking-unlocking mechanism.

Dislocation Motion in Icosahedral Al-Pd-Mn Single Quasicrystals

Quasicrystals do not show translational symmetry. Nevertheless, their plastic deformation at high temperatures is carried by dislocations. The first direct proof of the mobility of dislocations in quasicrystals was given by Wollgarten et al. (1995) by in situ straining experiments in the HVEM. In recent experiments (Messerschmidt et al., 1998a) the activated slip planes were identified as perpendicular to fivefold, threefold, and pseudo-twofold directions. Figure 9 shows an example of dislocations that moved on different slip planes. The planes can be determined from the slip traces the dislocations form during their motion. The dislocations are arranged in well-defined crystallographic directions, which, however, had not been observed in postmortem investigations (Rosenfeld et al., 1995). The directions determined so far are the twofold direction on the threefold plane, and a direction including an angle of about 60° with the twofold direction on the pseudo-twofold plane. These preferred orientations point to an intrinsic mechanism controlling the dislocation mobility. Feuerbacher et al. (1997) proposed that the interaction between the dislocations and the Mackay-type clusters is the rate-controlling process. These clusters are aligned along defined crystallographic directions in accordance with the preferred orientations of dislocations in the in situ experiments. Some of the present authors (Messerschmidt et al., 1998b) showed that a semiquantitative agreement between this model and the macroscopic activation parameters can only be obtained if the clusters are considered to be extended obstacles, in line with the theory of solution hardening of Labusch and Schwarz (1991).

An important problem in the deformation of quasicrystals is the origin of glissile dislocations. Figure 10 shows grown-in dislocations that moved over short distances as indicated by their slip traces. Usually, these dislocations do not move over long distances, as those in Figure 9 do. During the in situ experiments, many dislocations are generated in regions of stress concentrations, i.e., near cracks or the edges of the perforation of the specimens. In a few cases, dislocation generation was recorded on video tape. These records demonstrate that new dislocations can be created by gliding dislocations. Unfortunately, the details of this process could not be resolved until now. Nevertheless, the results of the in situ experiments contribute considerably to

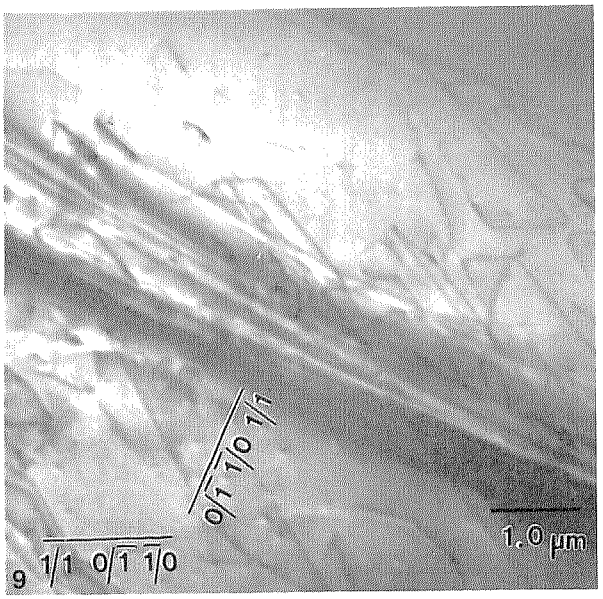

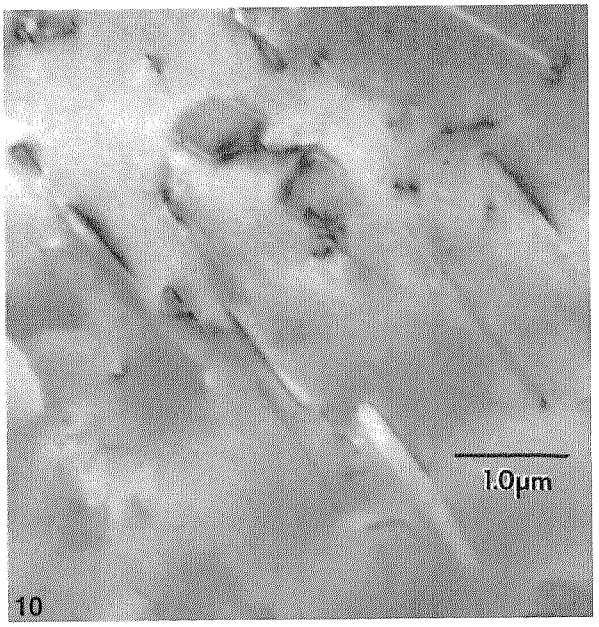

Figure 9. Dislocations in an Al-Pd-Mn single quasicrystal moving on different slip planes, characterized by their slip traces, during in situ deformation at about 750°C.

Figure 10. Grown-in dislocations in an Al-Pd-Mn single quasicrystal moving short distances during in situ deformation at about 700°C.

the understanding of the new phenomenon of plastic deformation of quasicrystals.

Conclusions

In situ straining experiments above 1000°C with a transmission electron microscope are feasible by using electron bombardment to heat the specimen grips. High-temperature straining experiments help to clarify a number of deformation processes in different types of materials.

1. Evidence was given for the first time of ferroelastic domain switching in partially stabilized zirconia. Ferroelastic deformation changes the microstructure for subsequent dislocation plasticity.
2. In the ODS alloy INCOLOY MA 956 at high temperatures, the waiting times of dislocations in configurations pinned by the oxide particles are of the same order of magnitude as the traveling times between these configurations. The respective friction mechanism has not been considered before.
3. In situ straining experiments on $MoSi_2$ single crystals showed the generation of dislocations on the $\langle 111 \rangle \{110\}$ slip system in localized sources and their viscous motion.
4. In situ straining experiments on Al-Pd-Mn single quasicrystals gave the first direct proof of dislocation motion in quasicrystals. In contrast to postmortem studies, they show dislocations under load aligned in crystallographic directions. This observation together with the viscous character of the dislocation motion help to understand the processes controlling the dislocation mobility in quasicrystals.

Acknowledgments

The authors thank Christian Dietzsch and Wolfgang Greie for keeping the Halle HVEM in very good condition and for technical help. They are also grateful to the Deutsche Forschungsgemeinschaft (DFG) and the Volkswagen-Stiftung for financial support.

References

Arzt E, Wilkinson DS (1986) Threshold stresses for dislocation climb over hard particles: the effect of an attractive interaction. *Acta Metall* 34:1893–1898

Baufeld B, Baither D, Messerschmidt U, Bartsch M (1995) High voltage electron microscopy *in situ* study on the plastic deformation of partially stabilized tetragonal zirconia. *Phys Status Solidi A* 150:297–306

Baufeld B, Baither D, Messerschmidt U, Bartsch M (1997) Ferroelasticity of t'-zirconia: II, *in situ* straining in a high-voltage electron microscope. *J Am Ceram Soc* 80:1699–1705

Chan CJ, Lange FF, Rühle M, Jue FF, Virkar AV (1991) Ferroelastic domain switching in tetragonal zirconia single crystals—microstructural aspects. *J Am Ceram Soc* 74:807–813

Feuerbacher M, Metzmacher C, Wollgarten M, Urban K, Baufeld B, Bartsch M, Messerschmidt U (1997) The plasticity of icosahedral quasicrystals. *Mater Sci Eng A* 233:103–110

Fujita H, Komatsu M (1983) In situ experiments of refractory materials at very-high temperatures. In: *Proc 7th Int Conf on High Voltage Electron Microscopy,* Fisher RM, Gronsky R, Westmacott KH (eds). Berkeley: University of California, pp 371–376

Heuer AH, Lanteri V, Dominguez-Rodriguez A (1989) High-temperature precipitation hardening of Y_2O_3 partially stabilized ZrO_2 (Y-PSZ) single crystals. *Acta Metall* 37:559–567

Ito K, Inui H, Shirai Y, Yamaguchi M (1995) Plastic deformation of $MoSi_2$ single crystals. *Phil Mag A* 72:1075–1097

Kiguchi T (1997) Study on phenomenon and mechanism of ferroelastic domain switching in partially stabilized zirconia crystals. *Preprint*

Labusch R, Schwarz RB (1991) Simulation of thermally activated dislocation motion in alloys. In: *Strength of Metals and Alloys,* Brandon DG, Chaim R, Rosen A (eds.). London: Freund Publications, pp 47–68

Messerschmidt U, Bartsch M (1994) High-temperature straining stage for in situ experiments in the high-voltage electron microscope. *Ultramicroscopy* 56:163–171

Messerschmidt U, Baither D, Baufeld B, Bartsch M (1997) Plastic deformation of zirconia single crystals: a review. *Mater Sci Eng A* 233:61–74

Messerschmidt U, Geyer B, Bartsch M, Feuerbacher M, Urban K (1998a) Dislocation motion in Al-Pd-Mn single quasicrystals. In: *Proc. 6th Int. Conf. on Quasicrystals, Tokyo 1997,* Takeuchi S, Fujiwara T (eds). Singapore: World Scientific, pp 509–512

Messerschmidt U, Bartsch M, Feuerbacher M, Geyer B, Urban K (1998b) Friction mechanism of dislocation motion in Al-Pd-Mn quasicrystals. *Phil Mag Lett,* in press.

Rosenfeld R, Feuerbacher M, Baufeld B, Bartsch M, Wollgarten M, Hanke G, Beyss M, Messerschmidt U, Urban K (1995) Study of plastically deformed icosahedral Al-Pd-Mn single quasicrystals by transmission electron microscopy. *Phil Mag Lett* 72:375–384

Schuster H, Herzog R, Czyrska-Filemonowicz A (1995) Iron-base oxide dispersion strengthened alloys: tensile and creep behaviour and its modelling. *Metall Foundry Eng* 21:273–286

Srolovitz DJ, Luton MJ, Petkovic-Luton R, Barnett DM, Nix WD (1984) Diffusionally modified dislocation-particle elastic interactions. *Acta Metall* 32:1079–1088

Valle R, Genty B, Marraud A, Cadoz J (1982) High temperature *in situ* experimentation in HVEM: instrumentation and application to materials science. In: *Electron Microscopy and Analysis 81, Inst. Phys. Conf. Ser. 61,* pp 35–38

Wollgarten M, Bartsch M, Messerschmidt U, Feuerbacher M, Rosenfeld R, Beyss M, Urban K (1995) *In-situ* observation of dislocation motion in icosahedral Al-Pd-Mn single quasicrystals. *Phil Mag Lett* 71:99–105